Phase Behavior of Lithium Perchlorate-Doped Poly(styrene-*b*-isoprene-*b*-ethylene oxide) Triblock Copolymers

Thomas H. Epps, III, Travis S. Bailey, Hoai D. Pham, and Frank S. Bates*

Department of Chemical Engineering and Materials Science, University of Minnesota, Minneapolis, Minnesota 55455

Received October 2, 2001. Revised Manuscript Received January 30, 2002

We report on the phase behavior of a system of lithium perchlorate-doped poly(styrene-*b*-isoprene-*b*-ethylene oxide) (SIO) triblock copolymers. Two complete phase diagrams are described along the isopleth formed by equal volume fractions of polystyrene and polyisoprene and varying poly(ethylene oxide) contents at ether oxygen-to-lithium ratios of 48:1 and 24:1 between 70 and 200 °C. Our results, based primarily on small-angle X-ray scattering (SAXS) data, reveal four phases as a function of PEO and salt content: two-domain lamellae (LAM_2), a pillared lamellar structure (PLS), core−shell cylinders (CSC), and three-domain lamellae (LAM_3). Two microstructures present in the neat material, core−shell gyroid (CSG), and semiperforated lamellae (SPL), are replaced by the CSC phase in the doped systems. In addition, the order−disorder transition temperatures at low PEO content increase dramatically with the addition of salt. Within the CSC phase, $LiClO_4$ can be dispersed up to a loading of 3:1 without inducing macroscopic phase separation. These findings are rationalized on the basis of the associated modifications to the three segment−segment interaction parameters and PEO chain statistics that accompany the selective mixing of $LiClO_4$ in the PEO domains, thereby driving microphase separation toward the strong-segregation limit.

I. Introduction

ABC triblock copolymers offer much richer phase behavior with a greater multitude of complex morphological structures than are available in their AB diblock counterparts. Diblock copolymer theory employs one segment−segment interaction parameter (χ_{AB}) and one independent composition parameter ($f_A = 1 - f_B$), along with the molecular weight. In linear ABC triblock copolymers, there are three segment−segment interaction parameters, (χ_{AB}, χ_{AC}, and χ_{BC}), two independent composition variables (f_A and f_B, with $f_C = 1 - f_A - f_B$), molecular weight, and three possible block sequences (ABC, BAC, and ACB). Today, each ABC triblock system has the potential to yield new and unexpected phases, greatly complicating the prediction of phase behavior using conventional mean-field theory.[1,2] Although these complexities make the task of systematic triblock characterization daunting, the rich phase space of ABC triblocks continues to motivate exciting research. Notable progress has been reported by a host of groups,[3−10] beginning in the 1980s with the works of Matsushita et al.,[11,12] followed by the influential studies of Stadler and co-workers,[13−15] and a recent example from our program.[16]

Recently, we initiated a systematic study of the poly(styrene-*b*-isoprene-*b*-ethylene oxide) (SIO) system,[17] focusing on a series of triblocks located along an isopleth in the pseudo-three component phase diagram. (For the remainder of this article, we refer to the individual polymers as PS, PI, and PEO but use the abbreviated forms SI, SO, IO, and SIO for the diblock and triblock copolymers.) To perform this study, the same parent SI diblock was used in the synthesis of each SIO triblock. The culmination of these experiments is shown in Figure 1a. Six distinct morphological regions are located in the composition range between the symmetric SI diblock and the symmetric ($^1/_3$:$^1/_3$:$^1/_3$) SIO triblock. These regions include two-domain lamellae (LAM_2), a pillared lamellar structure (PLS) (tentatively assigned), hexagonal core−shell cylinders (CSC), core−shell gyroid

* To whom correspondence should be addressed.

(1) Nakazawa, H.; Ohta, T. *Macromolecules* **1993**, *26*, 5503.
(2) Zheng, W.; Wang, Z. *Macromolecules* **1995**, *28*, 7215.
(3) Bates, F. S.; Frederickson, G. H. *Phys. Today* **1999**, *52*, 32−38.
(4) Gido, S. P.; Schwark, D. W.; Thomas, E. L.; do Carmo Goncalves, M. *Macromolecules* **1993**, *26*, 2636.
(5) Matsen, M. W. *J. Chem. Phys.* **1998**, *108*, 785−795.
(6) Abetz, V.; Stadler, R. *Macromol. Symp.* **1997**, *113*, 19.
(7) Arai, K.; Kotaka, T.; Kitano, Y.; Yoshimura, K. *Macromolecules* **1980**, *13*, 1670.
(8) Reiss, G.; Schleinger, M.; Marti, S. *Macromol. Sci.-Phys.* **1980**, *B17*, 355.
(9) Shibayama, M.; Hasegawa, H.; Hasimoto, T.; Kawai, H. *Macromolecules* **1982**, *15*, 274.
(10) Isono, Y.; Tanisuigi, H.; Endo, K.; Fujimoto, T.; Hasegawa, H.; Hasimoto, T.; Kawai, H. *Macromolecules* **1983**, *16*, 5.
(11) Matsushita, Y.; Chosi, H.; Fujimoto, T.; Nagasawa, M. *Macromolecules* **1980**, *13*, 1053.
(12) Matsushita, Y.; Tamada, K.; Hattori, T.; Fujimoto, T.; Sawada, Y.; Nagasawa, M.; Matsui, C. *Macromolecules* **1983**, *16*, 10.
(13) Auschra, C.; Stadler, R. *Macromolecules* **1993**, *26*, 6364.
(14) Auschra, C.; Stadler, R. *Macromolecules* **1993**, *26*, 2171.
(15) Stadler, R.; Auschra, C.; Neckmann, J.; Krappe, U.; Voigt-Martin, I.; Leibler, L. *Macromolecules* **1995**, *28*, 3080.
(16) Shefelbine, T. A.; Vigild, M. E.; Matsen, M. W.; Hajduk, D. A.; Hillmyer, M. A.; Cussler, E. L.; Bates, F. S. *J. Am. Chem. Soc.* **1999**, *121*, 8457.
(17) Bailey, T. S.; Pham, H. D.; Bates, F. S. *Macromolecules*, **2001**, *34*, 6994−7008.

10.1021/cm010971t CCC: $22.00
Published on Web 03/21/2002

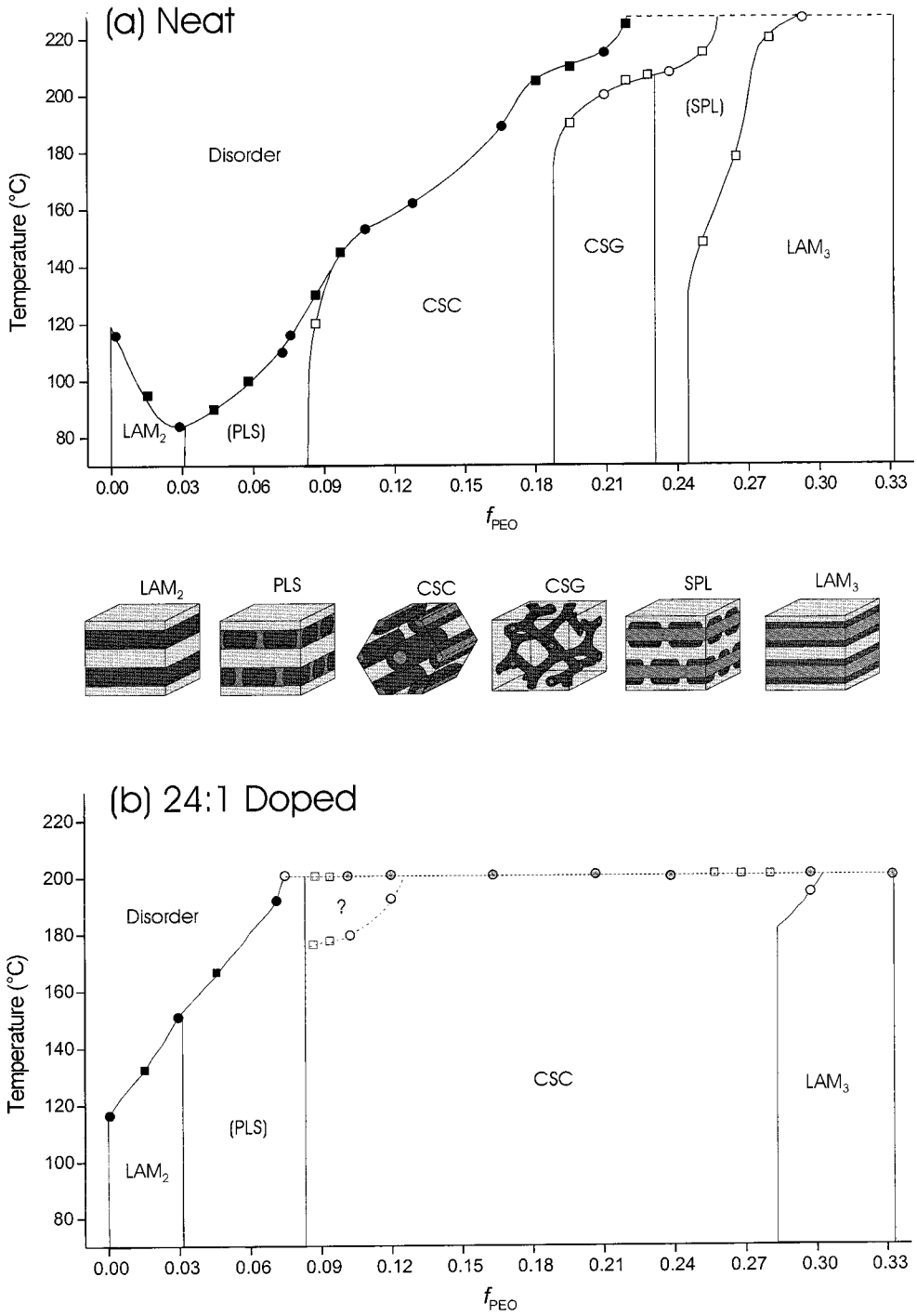

Figure 1. (a) Neat phase diagram adapted from Bailey et al.[17] detailing the structures found in the PS−PI−PEO triblock copolymer phase diagram. ● and ■ represent ODTs for neat triblock samples and triblock blends, respectively. ○ and □ represent OOTs for neat triblock samples and triblock blends, respectively. The dashed horizontal line at 225 °C represents the experimental ceiling. (b) Phase diagrams detailing the structures found in the lithium-doped SIO triblock isopleth system between the symmetric diblock and symmetric triblock states. ● and ■ represent ODTs for doped triblock samples and doped triblock blends, respectively. ○ and □ represent OOTs for doped triblock samples and doped triblock blends, respectively. ⊙ and ⊡ represent locations of doped triblock samples and doped triblock blends, respectively, at the experimental ceiling. The dashed horizontal line at 200 °C represents the experimental ceiling.

(CSG), three-domain semiperforated lamellae (SPL) (tentatively assigned), and three-domain lamellae (LAM_3). In the remaining sections of this article, we drop the qualifier "tentatively assigned" when referring to the PLS and SPL phases for brevity. In addition, Bailey et al. report that the blending of triblocks with similar composition does not have a significant effect on either the polymer morphologies or the location of order−order and order−disorder transition temperatures and compositions.[17]

In 1978, Armand suggested that polymers such as poly(ethylene oxide) (PEO) and poly(propylene oxide) (PPO) complexed with alkali metal salts could be useful as solid-state polymer electrolytes.[18] For these electrolytes, the transport property of greatest interest is the DC conductivity. Chandrasekhar and others have de-

termined that the conductivity of a solid PEO electrolyte is a function of the dissolved salt concentration; however, maximum conductivity occurs at intermediate salt concentrations, normally between [O]/[Li] molar ratios of 40:1 and 12:1.[19,20] Other parameters are at least as important when considering the overall design and performance of an electrochemical cell. These include the mechanical properties of the solid polymer electrolyte, the size and continuity of the porous spaces, and the interfacial stability between the electrode materials and the electrolyte under normal operating conditions. Unfortunately, many attempts to improve polymer ionic conductivity have resulted in poorer membrane mechanical properties.[21−27] A primary goal of this research program is to produce an ionically conductive block copolymer membrane with the nonconductive blocks selected to maintain membrane toughness and structural integrity.

Thus, our choice of a triblock copolymer containing PS, PI, and PEO was not arbitrary. PEO remains one of the most promising solid-state polymer electrolytes. This research explores the possibilities for employing triblock copolymers in applications such as conducting membranes through the creation of doped multicontinuous phases or through the electric-field or shear alignment of cylindrical or lamellar phases. The first step in this process is to establish the feasibility of selectively doping these triblock copolymers with ionic salts and characterizing the morphological consequences.

II. Experimental Section

Synthesis and Characterization of Poly(styrene-*b*-isoprene-*b*-ethylene oxide) (SIO) Triblock Copolymers. The synthesis of SIO triblock copolymers was accomplished through sequential anionic polymerization techniques. The initial polymerization steps involved the synthesis of a poly(styrene-*b*-isoprene) diblock end-capped with ethylene oxide to generate a hydroxyl end group. Subsequently, a series of triblocks was created by reinitiation of the diblock with potassium naphthalenide and additional ethylene oxide. In this way, a single batch of SI diblock was converted to ten SIO triblocks with PEO volume fractions ranging from 0 to 33.2%. Triblock copolymer compositions were determined by NMR spectroscopy, and the PEO volume fraction results are listed in Table 1; binary blends, denoted SIO*i*/*j*, where SIO*i* and SIO*j* are the constituents, are also identified in Table 1. Repeat unit mole fractions were calculated on the basis of relative peak intensities, and volume fractions were calculated using published homopolymer densities at 140 °C (ρ_{PS} = 0.969 g/cm^3, ρ_{PI} = 0.830 g/cm^3, ρ_{PEO} = 1.064 g/cm^3).[28] Density data were not corrected to reflect differences in temperature. A more detailed examination of the synthesis, characterization, and blending procedures can be found in ref 17, along with a description of the SIO nomenclature.

Table 1. Phase Behavior of Poly(styrene-*b*-isoprene-*b*-ethylene oxide)/$LiClO_4$ Mixtures

		[O]/[Li] = 48:1		[O]/[Li] = 24:1	
sample[a]	f_{PEO}	ODT[b] (°C)	morphology[c]	ODT[b] (°C)	morphology[c]
parent diblock	0.002	116	LAM_2 → DIS	116	LAM_2 → DIS
SIO0/2	0.014	129	LAM_2 → DIS	129	LAM_2 → DIS
SIO2	0.029	147	LAM_2 → DIS	149	LAM_2 → DIS
SIO2/4	0.046	157	PLS → DIS	164	PLS → DIS
SIO4	0.072	176	PLS → DIS	185	PLS → DIS
SIO1	0.077	180	PLS → DIS	−	PLS
SIO1/5a	0.084	−	CSC → ?	−	CSC → ?
SIO1/5b	0.097	−	CSC → ?	−	CSC → ?
SIO5	0.108	−	CSC → ?	−	CSC → ?
SIO3	0.125	−	CSC → ?	−	CSC → ?
SIO6	0.164	−	CSC	−	CSC
SIO7	0.207	−	CSC	−	CSC
SIO8	0.237	−	CSC	−	CSC
SIO8/9a	0.258	−	CSC	−	CSC
SIO8/9b	0.269	−	CSC	−	CSC
SIO8/9c	0.280	−	LAM_3	−	CSC
SIO9	0.293	−	LAM_3	−	LAM_3 → CSC
SIO10	0.332	−	LAM_3	−	LAM_3

[a] Notation SIO*i*/*j* represents a blend made from polymers SIO*i* and SIO*j*. [b] Unlisted ODT indicates that the transition temperature is greater than 200 °C. [c] DIS, disordered state; LAM_2, two-domain lamellae; PLS, pillared lamellae; CSC, hexagonal core−shell cylinders; LAM_3, three-domain lamellae.

Lithium Perchlorate Doping. Lithium perchlorate was obtained from Aldrich (99.5%) and used as received. A measured amount of triblock copolymer was dissolved in THF, followed by the addition of the salt. Samples were freeze-dried in either 2-mL ampules or 10-mL vials and stored under vacuum prior to use. To eliminate the possibility of solvent-induced morphological effects, the neat polymer specimens were subjected to the same treatment. We note that the results reported here, generated from samples recovered from THF, are indistinguishable from those presented by Bailey et al.[17] based on recovery from benzene. Thus, we can safely ignore solvent effects during freeze-drying.

Small-Angle X-ray Scattering (SAXS). SAXS experiments were conducted at the University of Minnesota Institute of Technology (IT) characterization facility. For these experiments, 1.54-Å Cu Kα X-rays were generated using a Rigaku RU-200BVH rotating anode equipped with a 0.2 × 2 mm microfocus cathode and total reflecting Franks mirror optics. 2D-SAXS data were collected on a Siemens HI-STAR multiwire area detector. Samples were placed within an evacuated chamber/tube assembly and maintained at the desired temperature by a pair of water/glycol-cooled block heaters. All SAXS data presented in this report were corrected to eliminate detector response characteristics and plotted on a logarithmic scattering intensity axis versus the magnitude of the scattering vector, $|\mathbf{q}|$

$$|\mathbf{q}| = q = \frac{4\pi}{\lambda}\sin\left(\frac{\theta}{2}\right)$$

where θ is the scattering angle between the incident and scattered radiation. Furthermore, because of the isotropic nature of the samples tested in this work, all 2D scattering patterns could be azimuthally integrated to the one-dimensional form of intensity versus q.

Dynamic Mechanical Spectroscopy (DMS). Spectroscopy experiments were conducted on a Rheometrics Scientific

(18) Armand, M. B.; Chabagno, J. M.; Duclot, M. *Second Int. Meet. Solid Electrolytes* **1978**, *20−22*, 131−136.
(19) Robitaille, C. D.; Fauteux, D. *J. Electrochem. Soc.* **1986**, *133*, 315−325.
(20) Chandrasekhar, V. *Adv. Polym. Sci.* **1998**, *135*, 139−205.
(21) Gray, F. M. *Solid Polymer Electrolytes: Fundamentals and Technological Applications*; VCH Publishers: New York, 1991; Chapter 6.
(22) Xia, D. W.; Soltz, D.; Smid, J. *Solid State Ionics* **1984**, *14*, 221.
(23) Kobayashi, N.; Ushiyama, M.; Tsuchiuda, E. *Solid State Ionics* **1985**, *17*, 307.
(24) Bannister, D. J.; Davies, G. R.; Ward, I. M.; MacIntyre, J. E. *Polymer* **1984**, *25*, 1600.
(25) Ding, L. *Polym. Bull.* **1996**, *37*, 639.
(26) Blonksy, P. M.; Shriver, D. F.; Austin, P.; Allcock, H. R. *J. Am. Chem. Soc.* **1984**, *106*, 6854.
(27) Fauteux, D.; Massucco, A.; McLin, M.; Van Buren, M.; Shi, J. *Electrochim. Acta* **1995**, *40*, 2185.
(28) Fetters, L. J.; Lohse, D. J.; Ritcher, D.; Witten, T. A.; Zirkel, A. *Macromolecules* **1994**, *27*, 4639−4646.

ARES strain-controlled rheometer using a parallel-plate configuration with 25-mm-diameter plates. DMS was useful for determining the approximate temperatures where triblock copolymers undergo order−order and order−disorder transitions (OOTs and ODTs, respectively). Isochronal ($\omega = 1$ rad/s) temperature ramps at constant heating rate (between 1 and 6 °C/min) were conducted to measure the dynamic elastic (G') and loss (G'') moduli. The experiments were run in a nitrogen-filled chamber to minimize sample oxidation at elevated temperatures. Strain amplitudes (0.5−3.0%) were chosen such that all temperature ramp measurements were conducted in the linear viscoelastic region. Sample T_{ODT}s on heating were defined by sudden, large decreases in the dynamic moduli, and all heating T_{ODT}s were verified by their reproducibility upon cooling.

One-mm-thick polymer specimens were prepared by placing freeze-dried samples in a metal mold and hot pressing at 750 psi for 8−10 min. All samples were pressed at approximately 100 °C. Bailey et al. state that they pressed samples at temperatures approximately 15 °C above the T_{ODT};[17] however, that method was not followed in this project to minimize possible degradation of the PEO block when doped with lithium perchlorate.[19,29]

DMS was an important tool in the determination of phase boundaries in the lithium-doped SIO phase diagram, indicating the locations of both order−order and order−disorder transitions. In all cases, at the slower heating and cooling rates of 1−2 °C/min, the hysteresis between heating and cooling ODTs was limited to 1−5 °C. Furthermore, all T_{ODT} values presented in this report were obtained from the heating runs, and each run was repeated to ensure that the sudden drop in elastic moduli was caused by a phase transition to a disordered state, as opposed to polymer degradation. The order−order and order−disorder transition data were corroborated by SAXS measurements.

III. Results and Analysis

SIO triblock copolymers were doped with lithium perchlorate salt at concentration ratios of main-chain oxygen to lithium ([O]/[Li]) ranging from 48:1 to 1:1. Additional specimens with intermediate PEO contents were created by blending triblocks of marginally different compositions prior to the addition of salt. This blending method, validated by Bailey et al. in a previous publication,[17] provides an efficient method for expanding the resolution of the study. The remainder of this section is divided into five parts, each detailing a separate aspect of our investigation.

Polymer Morphology as a Function of Salt Concentration. The establishment of polymer morphological integrity in the range of doping compositions required for optimal conductivity was a necessary component of this study. Figure 2a shows a representative SAXS concentration ramp for SIO3 (12.5% PEO by volume), exhibiting the stability of the hexagonal core−shell cylinder (CSC) phase at increasing salt concentrations. (Although the first peak is absent in the neat material, the hexagonal CSC assignment was confirmed by TEM analysis.[17]) Distinct peaks are visible at salt compositions ranging from 48:1 to 3:1. Thus, the CSC phase remains intact at salt concentrations necessary for optimal conductivity. Furthermore, the gradual formation of $\sqrt{7}q^*$ and $\sqrt{9}q^*$ peaks occurs as the salt composition increases (where q^* is the location of the leading reflection).

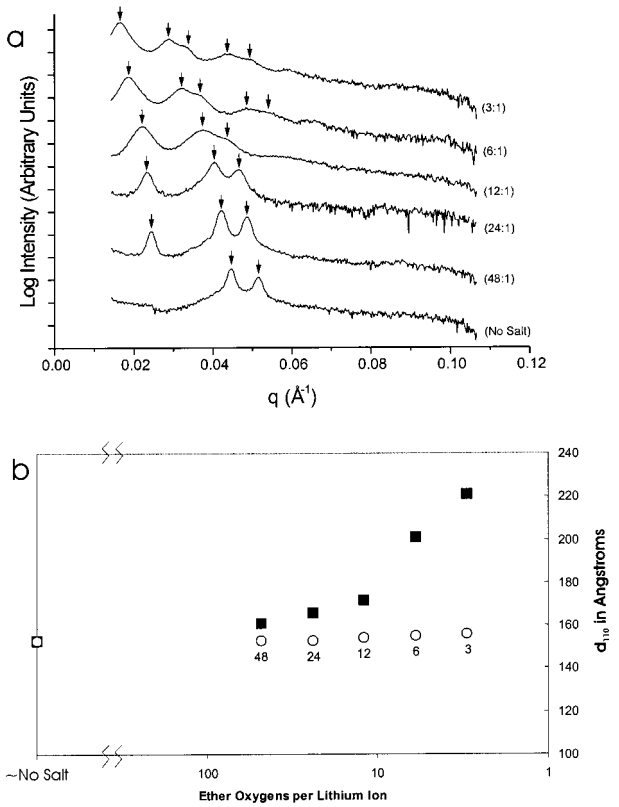

Figure 2. (a) SAXS data (100 °C) from experiments on SIO3 samples. Relative positions of the diffraction peaks, identified by arrows, are consistent with the core−shell cylinder (CSC) morphology. The scattering patterns were progressively shifted vertically. (b) Plot of d_{110} domain spacing as determined by SAXS data (100 °C) from experiments on SIO3 samples. ■ represents actual SAXS data. ○ represents the estimated domain spacings determined on the basis of the ideal mixing of PEO and $LiClO_4$.

Several other features are evident in Figure 2: The peak resolution decreases with increasing salt concentration, accompanied by lower q values for all peaks (see Figure 2b for the associated lattice spacing, d_{110}). Figure 2b shows d_{110} values calculated on the basis of estimated (ideal) lattice expansion due to the volume of added lithium perchlorate salt. Clearly, the additional volume of $LiClO_4$ is not solely responsible for the shift in peak locations.

The 1:1 samples, the highest salt concentration examined, showed disruption of the CSC and LAM_3 phases. Evidence of phase separation was obtained from SAXS profiles (not pictured), where the diffraction patterns do not resemble those seen at lower lithium concentrations. We did not attempt to evaluate the 1:1 specimens in detail as the lithium concentration was much higher than the levels necessary for optimal conductivity.[20]

Polymer Morphology as a Function of Temperature. The effect of temperature on morphology was also studied, and representative SAXS results were compared at temperatures from 70 to 200 °C for SIO6 (16.4% PEO by volume) at a lithium composition of 24:1 (not pictured). Heating and cooling runs were performed and provided identical results, indicating the reversibility and equilibrium state of the system. The scattering patterns demonstrated the stability of the lithium-doped hexagonal CSC morphology at elevated tempera-

(29) Jacobs, P. W. M.; Lorimer, J. W.; Russer, A.; Wasiucionek, M. *J. Power Sources* **1989**, *26*, 503−510.

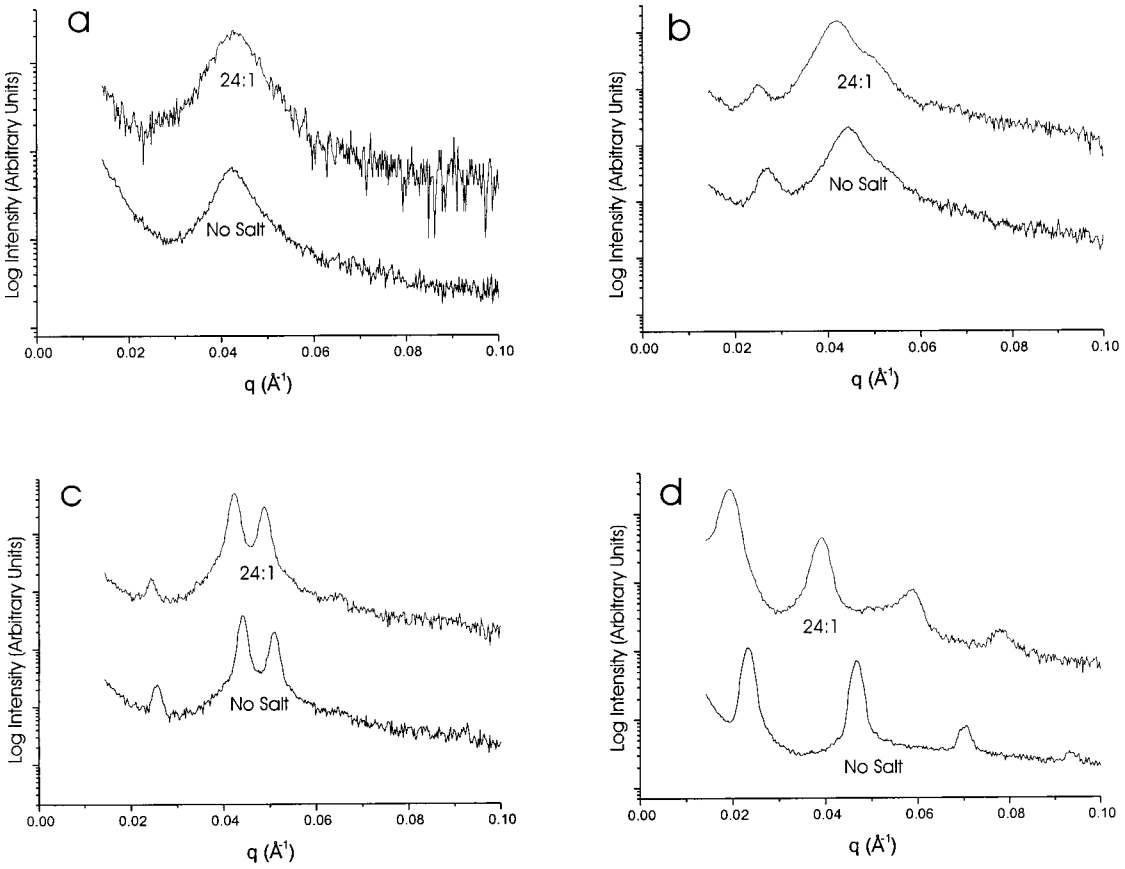

Figure 3. (a) SAXS data (70 °C) from experiments on SIO2 and SIO2 (24:1). (b) SAXS data (100 °C) from experiments on SIO1 and SIO1 (24:1). (c) SAXS data (110 °C) from experiments on SIO5 and SIO5 (24:1). (d) SAXS data (120 °C) from experiments on SIO10 and SIO10 (24:1). Upper traces in each panel have been displaced vertically.

tures and revealed a minimal shift in peak locations as the temperature increased. In addition, Bragg peak definition increased somewhat as the temperatures rose. This trend was most noticeable in the heating and cooling runs for the $\sqrt{3}q^*$ and $\sqrt{4}q^*$ peaks. Finally, even though the ODT was not accessed in the doped SIO6 material, the sample exhibited a CSC morphology above the ODT of the comparable neat material (~189 °C). This trend was documented in all samples and will be considered again in the following sections.

Polymer Morphology as a Function of PEO Volume Fraction. The effect of PEO volume fraction on lithium-doped SIO triblock copolymers was studied, and representative SAXS patterns are shown in Figure 3 for neat and 24:1 samples. Figure 3a shows results for an SIO2 (2.9% PEO by volume) sample in the doped and neat states. The doped results are essentially identical to those reported by Bailey and co-workers, who identified this morphology as two-domain lamellar (LAM_2) using TEM and SAXS.[17] SAXS data for all samples in this region gave very strong q^* peaks; however, the $2q^*$, $3q^*$, and higher-order reflections were not detected. For the 24:1 system, this region spans a composition range of 0−3.1% PEO by volume, including the parent diblock, SIO0/2, and SIO2 samples.

Figure 3b shows representative SAXS data obtained from neat and doped SIO4 (7.2% PEO by volume) samples. Again, the SAXS patterns for the two samples are nearly identical, indicating a common morphology. Bailey et al. tentatively identified this morphology as a pillared lamellar structure (PLS), where PEO pillars lie within PI layers that are sandwiched between layers of PS.[17] These SAXS patterns exhibit two distinctive peaks located at q^* and $1.67q^*$. For the 24:1 oxygen/lithium system, this region exists over a composition range of 3.1−8.1% PEO by volume. The triblock samples located in this structural regime were SIO2/4, SIO4, and SIO1.

Figure 3c depicts SAXS plots for neat and doped SIO5 (10.8% PEO by volume) samples. Both SAXS patterns are consistent with a hexagonally packed core−shell cylindrical morphology with Bragg peaks located at q^*, $\sqrt{3}q^*$, $\sqrt{4}q^*$, $\sqrt{7}q^*$, and $\sqrt{9}q^*$. TEM images provided by Bailey and co-workers confirmed this morphological assignment in the unmodified sample.[17] The PEO blocks form cylindrical cores, which are encased in PI shells and embedded in a PS matrix. For the 24:1 oxygen/lithium system, this region occurs between 8.1 and 28.5% PEO by volume. The triblock samples located in this regime are SIO1/5a, SIO1/5b, SIO5, SIO3, SIO6, SIO7, SIO8, SIO8/9a, SIO8/9b, and SIO8/9c.

Figure 3d shows sample SAXS patterns obtained from SIO10 (33.2% PEO by volume) in the doped (24:1) and nondoped states. Again, aside from a shift in the relative peak positions, the lithium-doped SAXS pattern is essentially identical to the neat one, indicating a common morphology. Bailey et al. identified this morphology as three-domain lamellar (LAM_3) on the basis of TEM images and the diffraction peaks located at q^*, $2q^*$, $3q^*$, and higher. TEM showed that this morphology is supported by a head-to-head, tail-to-tail orientation of the polymer molecules (i.e., ABCCBA).[17] For the 24:1 oxygen/lithium system, LAM_3 exists within a composi-

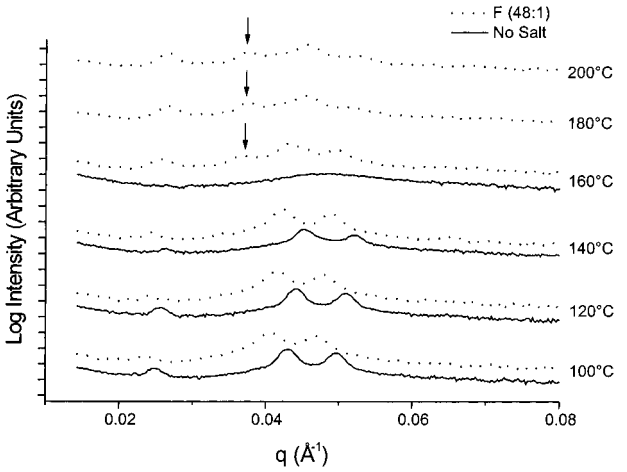

Figure 4. Comparison of SAXS results for neat (solid curves) and doped (24:1; dashed curves) versions of SIO5. Loss of distinct reflections between 140 and 160 °C in the neat specimen is associated with disordering. Order persists to at least 200 °C in the doped specimen. Development of a new reflection at 160 °C and above, identified by the arrow, might signify the formation of a new phase.

tion range of between 28.5 and 33.2% PEO by volume (symmetric SIO triblock). The samples located in this regime are SIO9 and SIO10. The phase space that extends past the symmetric triblock was not studied.

Order−Disorder Transition. The addition of lithium perchlorate has a pronounced effect on the order−disorder transition temperature determined by SAXS and DMS measurements. Figure 4 shows a representative SAXS pattern of SIO5 (10.8% PEO by volume) in the doped and neat states. The unmodified sample transitions from an ordered to a disordered state between 140 and 160 °C, as evidenced by the loss of multiple reflections at the higher temperatures, whereas order persists in the doped sample up to at least 200 °C. Ruzette et al. also found significant increases in the order−disorder transition temperature upon the addition of modest salt amounts to their POEM-containing diblock copolymers.[30]

DMS results obtained from neat and doped (48:1) SIO1 (7.7% PEO by volume) samples are presented in Figure 5. The unmodified sample exhibits a steep decline in G' ($\omega = 1$ rad/s) beginning at about 115 °C, which we associate with T_{ODT}. Just 1 lithium ion per 48 oxygen atoms elevates this phase transition temperature to around 180 °C. The doped sample shows a small hump at approximately 168 °C; closer analysis by DMS and SAXS indicated that this feature was reproducible and was not the result of an order−order transition. Table 1 lists T_{ODT} values for the 48:1 and 24:1 mixtures between 0 and 7.7% PEO by volume. Interestingly, doubling the salt content had only a modest effect on this phase transition temperature.

Lithium-Doped SIO Phase Diagram Isopleth. Phase diagrams for the lithium-doped SIO isopleth were constructed from the SAXS and DMS analysis of 10 SIO triblock copolymers and 7 SIO triblock blends. Using the temperature and concentration ramps previously discussed along with varying PEO volume fractions,

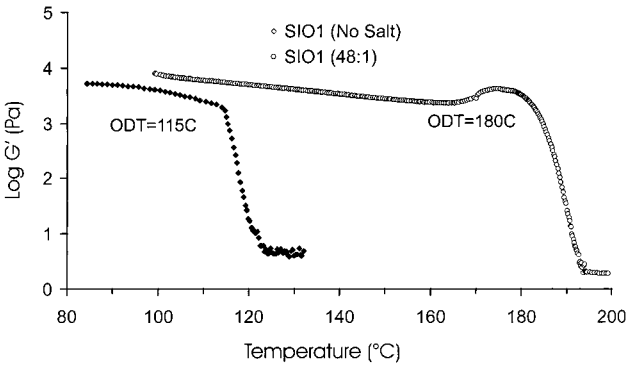

Figure 5. DMS data from experiments on SIO1 (neat) and SIO1 (48:1). Data show elastic modulus (G') measured during isochronal temperature ramps ($\omega = 1$ rad/s) at a heating rate of 1.5 °C/min. Both results are interpreted as a PLS-to-disorder transition.

pseudo-three-component isopleths were created for each lithium salt composition. Figure 1b shows an isopleth (T versus f_{PEO}) for the 24:1 system. The horizontal dashed line at 200 °C represents the upper boundary of data collection, set to limit degradation in the PEO/lithium-doped materials. The lower bound on measurements was 70 °C, just above the crystallization temperature of the PEO segments ($T_m \approx 65$ °C). The horizontal axis depicts the volume fraction of PEO present in the triblock copolymer, running from 0% in the SI diblock to 33.2% PEO by volume in the final SIO triblock.

The lithium-doped phase diagram isopleth shows the locations of the four morphologies identified during this program. In order of appearance, the four morphologies are two-domain lamellae, pillared lamellae, core−shell cylinders, and three-domain lamellae. Core−shell gyroid (CSG) and semiperforated lamellae (SPL), present in the diagram reported by Bailey et al. (see Figure 1a),[17] were not found in the lithium-doped phase diagram. A comparison between Figure 1a and 1b shows that the CSC morphology has displaced the regions occupied by the CSG and SPL structures in the neat material. This trend was observed in all of the phase diagrams with salt concentrations of 48:1 and higher.

The introduction of lithium perchlorate salt into the PEO domains shifts the balance of forces necessary for the formation of a stable CSG phase. A sample concentration ramp for SIO7 (20.7% PEO by volume) illustrating the disappearance of the CSG phase is shown in Figure 6. Two temperatures are represented in this figure, 180 and 200 °C. At 200 °C, all samples exhibit a hexagonal CSC morphology with a shift to larger domain spacings apparent as the salt concentration increases (this shift to larger domain spacings was also observed by Ruzette et al. for their POEM diblock copolymers). [30] This spacing change constitutes a 33% lattice expansion in the presence of just 1 lithium atom per 24 backbone oxygen atoms. In addition, $\sqrt{7}q^*$ and $\sqrt{9}q^*$ peaks are observed in both the 48:1 and 24:1 doped samples. At 180 °C (i.e., below the CSG → CSC transition in Figure 1a), the addition of a small amount of salt (48:1) promotes a transition to the core−shell cylinder phase, as evidenced by a distinct change in SAXS reflections. Here again, the system thermodynamics appears to be remarkably sensitive to small amounts of salt.

(30) Ruzette, A. G.; Soo, P. P.; Sadoway, D. R.; Mayes, A. M. *J. Electrochem. Soc.* **2001**, *148*, A537-A543.

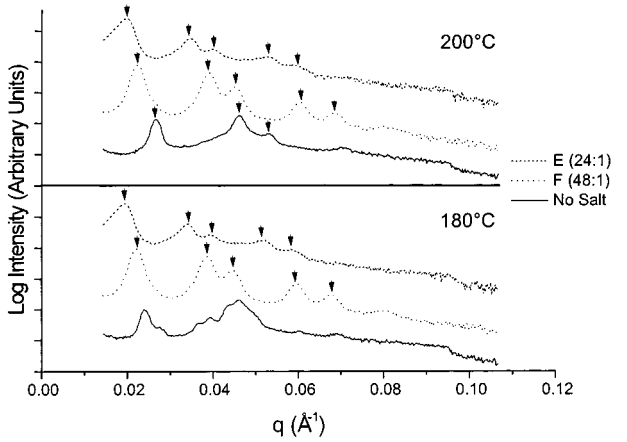

Figure 6. SAXS data from SIO7 (neat), SIO7 (48:1), and SIO7 (24:1) at 180 and 200 °C. Data from the neat sample (SIO7) at 180 °C are consistent with the core−shell gyroid (CSG) region in Figure 1a. At 200 °C, this sample lies in the CSC region in Figure 1a. Salt doping converts the CSG to CSC, as indicated by the SAXS results displayed in the lower panel.

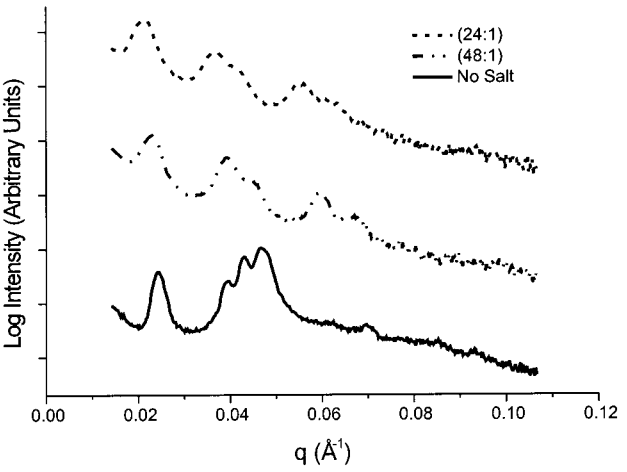

Figure 7. SAXS data (200 °C) from experiments on SIO8 (neat), SIO8 (48:1), and SIO8 (24:1). Neat sample data (SIO8) are consistent with the semiperforated lamellar (SPL) morphology depicted in Figure 1a. Lithium-doped sample data (SIO8, 48:1 and 24:1) are consistent with the CSC morphology in Figure 1b.

A similar situation occurs for the SPL region shown in Figure 1a. Bailey and co-workers rationalized the existence of the SPL phase as a manifestation of the frustration created by the tendency for the PEO block to interact with the PS block despite being physically connected to the PI block.[17] Loss of this morphology with the addition of salt is illustrated in Figure 7 (SIO8, 23.7% PEO by volume). The neat sample produces a distinctive SAXS pattern associated with the perforated lamellar morphology,[17] whereas the lithium-doped samples (48:1 and 24:1) show Bragg peaks indicative of a hexagonally packed CSC morphology.

A possible order−order transition was located in Figure 1b at elevated temperatures in the 24:1 system between 8.1 and 13.0 vol % of PEO. The associated high-temperature ordered phase is characterized by the reversible appearance of a new reflection (at $\sqrt{2}q^*$) in the SAXS patterns upon heating from the CSC state, as illustrated in Figure 5. There is insufficient information to make a morphology assignment solely on the basis of these data. The phase diagram isopleths for higher salt concentrations show an increase in the measurable OOTs and ODTs, as well as an expansion of the CSC region at the expense of the LAM_3 region.

IV. Discussion

We have presented data substantiating the existence of four morphologies (LAM_2, PLS, CSC, and LAM_3) between a parent SI diblock copolymer (0% PEO) and a series of lithium perchlorate-doped SIO triblock copolymers (up to 33.2% PEO by volume). A complete phase diagram isopleth was established between 70 and 200 °C for the lithium concentration ([O]/[Li]) of 24:1 in Figure 1b. (At 48:1, nearly the same phase diagram was recorded, as summarized in Table 1.) Also, sizable quantities of salt, up to an [O]/[Li] ratio of 3:1, were shown to be dispersible in the CSC phase, spanning the range required for optimal ionic conductivity.[19,20] Finally, addition of $LiClO_4$ significantly elevates the order−disorder transition temperature (T_{ODT}). We examine and rationalize these results in the following paragraphs in terms of our current understanding of block copolymer thermodynamics.

That moderate amounts of $LiClO_4$ can be mixed with PEO is now well established.[19,20,29,31−33] Robitaille and Fauteux[19] report a phase diagram revealing a eutectic point at about 50 °C and 0.2 weight fraction salt. Above the melting temperature of PEO, around 65 °C, a wide range of salt compositions can be accessed, up to approximately [O]/[Li] = 6. Above this concentration several phases coexist in equilibrium, including [O]/[Li] = 3, [O]/[Li] = 6, solid $LiClO_4$, and a homogeneous liquid mixture. The compound states at 3 and 6 backbone oxygen atoms per lithium atom are associated with specific coordination conditions that also influence ionic conductivity.[20] Although most of our experiments dealt with mixtures well within the homogeneous liquid-phase region, experiments with the CSC phase (Figure 2) suggest that the salt can be loaded into the PEO microdomains over the same concentration regime as reported for pure PEO.[19] At this point, we cannot state with certainty whether this reflects a set of true thermodynamic conditions or the suppression of nucleation and growth of macroscopic phases from the initial microphase-separated state. Nevertheless, confinement of PEO in nanometer-scale domains does not appear to hinder doping with conductive salt. This conclusion is supported by several other reports dealing with block copolymers.[30]

The effects produced by adding $LiClO_4$ to the SIO triblock copolymers can be traced primarily to changes in the χ parameters that control phase behavior and microdomain structure. Although we cannot make a quantitative estimate, salt of almost any kind should increase the degree of segregation between the PEO and PS or PI blocks, driving the material toward the strong-segregation limit. Consistent with this line of reasoning, we see the domain spacing increase (i.e., q^* decrease) with increasing salt content through the traces in

(31) Andreev, Y. G.; Bruce, P. G. *Electrochim. Acta* **2000**, *45*, 1417−1423.
(32) Wieczorek, W.; Raducha, D.; Zalewska, A.; J. R., S. *J. Phys. Chem. B* **1998**, *102*, 8725−8731.
(33) Kato, Y.; Watanabe, M.; Sanui, K.; Ogata, N. *Solid State Ionics* **1990**, *40/41*, 632−636.

Figures 2, 6, and 7. The unit cell dilation evident in these results, a 45% increase in d_{110} ($d_{110} = 2\pi/\sqrt{3}q^*$) between the neat and 3:1 specimens in Figure 2b, far exceeds that associated with the added volume of salt. Instead, we interpret this result in terms of a reduction in interfacial area at the expense of increased chain stretching, the classical balance between enthalpic and entropic factors that establishes the minimum Gibbs free energy in any block copolymer system.[5] Thus, we identify inflated effective χ parameters, $\chi_{eff,\,SO}$ and $\chi_{eff,\,IO}$, as contributing to the thermodynamics of the SIO/$LiClO_4$ system. From diblock copolymers in the SSL we expect $d^* \sim \chi^{1/6}$, implying that $\chi_{eff} \approx 9.1\chi$ at the 3:1 condition and 1.4χ at the 24:1 condition, provided that this is the only factor controlling chain stretching (see below).

The SAXS patterns in Figure 2a exhibit another interesting feature. As the salt concentration increases at constant temperature, the Bragg peaks associated with the CSC structure broaden because of coordinations between lithium cations and ether groups in the PEO blocks. Such ionic interactions between the cations and the unpaired electrons on the oxygen atoms are believed to function as transient cross-links, reducing the chain motion and increasing the effective polymer chain rigidity.[19,33,34] Solid-state NMR studies support these conclusions.[35] This also might contribute to the extraordinary degree of lattice expansion with added salt evident in Figure 2a and 2b. Lithium coordination likely stiffens the polymer backbone thereby increasing the effective statistical segment length, which impacts the lattice parameters directly. Because we lack sufficient understanding of how added salt modifies χ, we cannot quantify the separate roles of χ_{eff} and coordination-induced chain stiffening in the documented lattice expansion.

Elevated χ_{eff} values (and perhaps chain stiffening) also are consistent with the apparent loss of two morphologies in moving from the neat (Figure 1a) to the doped (Figure 1b) material. Although we are not aware of any theoretical efforts on triblocks that deal explicitly with segregation strength, comprehensive calculations by Matsen[36] on diblocks have shown a loss of the gyroid phase as the strong-segregation limit is approached. Apparently this trend applies to triblocks as well, at least within certain limits. The addition of just 1 lithium ion (and the corresponding perchlorate counterion) per 48 oxygen atoms is sufficient to eliminate the core−shell gyroid (CSG) and semiperforated lamellar (SPL) phases over the entire experimental parameter space. These morphologies are sacrificed in favor of the core−shell cylinder (CSC) phase. Curiously, the pillared lamellar structure (PLS) appears to be unaffected by doping (see below).

Doping affects the order−disorder transition temperature as well. In the neat material, T_{ODT} first decreases, to a minimum at $f_{PEO} = 0.03$, and then increases smoothly up to $f_{PEO} = 0.21$, where it hits 225 °C; above this composition, T_{ODT} exceeds our temperature window. Doping changes this behavior dramatically. First, the distinctly convex shape of $T_{ODT}(f_{PEO})$ transforms to a nearly linear form, leading to an increase of 60−70 °C in the disordering temperature at $f_{PEO} = 0.08$. Remarkably, this change is rather insensitive to doubling of the salt content from [O]/[Li] of 48:1 to 24:1. We believe that these modifications can also be attributed to an increased segment−segment interaction parameter.

Bailey et al.[17] rationalized the unusual dip in T_{ODT}-(f_{PEO}) in terms of the tendency for the PS blocks to make contact with PEO blocks. This is a natural consequence of $\chi_{SO} < \chi_{IO}$; however, it conflicts with the block sequencing imposed by the synthetic procedures. As small PEO blocks are added to the SI parent diblock, the more favorable PS/PEO contacts can be realized provided the material is disordered. Once the PEO block becomes large enough, it is forced to segregate. Struts that span the PI layers afford some contact between PEO and PS (see PLS morphology in Figure 1) despite the state of order. Surprisingly, the addition of salt does not seem to affect this sequence of phases with increasing PEO content, although it does eliminate the convex shape of the ODT. Presumably, the tendency to make PS/PEO contacts remains active, hence preserving the PLS phase, whereas the state of disorder is overwhelmed by the increased magnitude of both χ_{SO} and χ_{IO} in the presence of $LiClO_4$. The proximity of the PLS phase to T_{ODT} also might contribute to its retention with doping, compared with the loss of the CSG and SPL phases, which reside at stronger states of segregation in our system.

Another unusual feature displayed by the doped blends is revealed by reviewing SAXS temperature ramps. SAXS data taken from sample SIO6 with a 24:1 salt loading, located in the center of the CSC region in Figure 1b, appear to improve in resolution as the temperature is increased, particularly as evidenced by the second- and third-order reflections. Conventionally, the opposite occurs, unless the material exhibits a lower ordering transition temperature, which is clearly not the case here. Chandrasekhar[20] and Watanabe et al.[33] make the interesting observation that ion aggregation in lithium-modified PEO increases (i.e., dissociation decreases) with increasing temperature. Cooling from elevated temperatures will be accompanied by progressively more transient cross-linking that can bind the PEO chains, drastically reducing mobility and possibly resulting in glassy-like behavior. Any associated microdomain distortion would reduce long-range order, and this might account for the change in peak resolution documented in the SAXS results.

The results presented here indicate the potential for creating ionically conducting membranes using ABC triblock copolymers. Ideally, we would like to access triply periodic and multicontinuous morphologies that do not require microdomain alignment to achieve maximum transport. Our evaluation of the phase diagrams in Figure 1a and 1b leads us to conclude that a reduction in the molecular weight in the SIO system, an inversion of the block sequence to ISO, or the selection of other less-incompatible blocks might lead to the recovery of the CSG or other network morphologies, by analogy with conventional block copolymer systems.

(34) Wolfenson, A. E.; Torresi, R. M.; Bonagamba, T. J.; De Paoli, M. A.; Panepucci, H. *J. Phys. Chem. B.* **1997**, *101*, 3469−3473.
(35) O'Gara, J.; Nazri, G.; MacArthur, D. *Polym. Prepr.* **1990**, *31*, 159−160.
(36) Matsen, M. W.; Bates, F. S. *Macromolecules* **1996**, *29*, 1091−1098.

V. Conclusion

We have demonstrated that SIO triblock copolymers can be doped with lithium perchlorate over a wide range of compositions. Selective mixing of this salt with the PEO blocks significantly modifies the phase behavior, leading to the loss of certain ordered morphologies [core−shell gyroid (CSG) and semiperforated lamellae (SPL)] with the expansion of core-shell cylinders (CSC) and the preservation of two-domain and three-domain lamellae (LAM_2 and LAM_3, respectively) and the pillared lamellar structure (PLS). An increase in the order−disorder transition temperature and expansion of ordered microdomain lattices were also documented. Our experiments indicate that sizable amounts of $LiClO_4$, ranging up to a 3:1 ratio of ether oxygen atoms to lithium ions, can be incorporated within the PEO domains. Modifications of the phase behavior with addition of salt can be rationalized on the basis of increases in the effective segment−segment interaction parameters and possibly the PEO block stiffening due to multichain coordination with lithium ions. These levels of doping, which cover the amounts associated with peak conductivity, are consistent with the accepted phase diagram for PEO (homopolymer) and $LiClO_4$, demonstrating that nanoscale domain formation in triblock copolymers is not a limitation in developing ionic conductors.

Acknowledgment. This work was supported by the NSF (DMR-9905008) and the Lucent Technologies CRFP Fellowship Program. The MRSEC program at the University of Minnesota is also acknowledged for equipment support.

CM010971T